Chemical Engineering and Communication, Vol. 120, pp. 45-58, Feb. 93

Chem. Eng. Comm. 1992, Vol. 00, pp. 000–000
Reprints available directly from the publisher.
Photocopying permitted by license only.

Printed in the United States of America

EFFECTIVE THERMAL CONDUCTIVITY OF BINARY MIXTURES AT HIGH SOLID TO GAS CONDUCTIVITY RATIOS

P. ADNANI,† I. CATTON, A.R. RAFFRAY and M.A. ABDOU

Mechanical, Aerospace and Nuclear Engineering Department,
University of California, Los Angeles,
Los Angeles, CA, 90024

(Received February 14, 1992; in final form July 23, 1992)

The effective thermal conductivity of single size and binary mixtures of packed particle beds with stagnant gas at high solid/gas conductivity ratios is determined by a deterministic, unit cell approach. The model results are shown to be in good agreement with experimental data for various gas pressures and solid to gas thermal conductivity ratios up to 1300. A set of correlations for effective conductivity of binary mixtures as a function of gas pressure and particle size is derived. The effect of particle swelling on the effective conductivity of binary mixtures is studied by performing a parametric study of the contact area between the particles.
KEYWORDS Thermal conductivity Binary mixtures High solid-to-gas conductivity ratios Influence of gas pressure Correlation for binary mixtures.

1. INTRODUCTION

The subject of heat and mass transport inside a packed bed with a stagnant fluid has received a great deal of attention in the past because of its importance in many engineering and physical situations (Cheng 1978, Luikov 1980, Friedman 1986, Torquato 1987, and Sommerton and Robers 1988). In design of insulating materials, packed bed chemical reactors, and while considering heat losses from buried nuclear waste, a good knowledge of effective thermal conductivity (k_e) of porous media is required. Sphere-pac fuels have been recommended as alternatives to cylindrical rods in light water reactors (LWR) and liquid-metal fast breeder reactors (LMFBR).

Another application of packed beds can be found in the field of thermonuclear fusion. Abdou *et al.* (1989) have suggested that for the ITER (International Thermonuclear Experimental Reactor) solid breeder blanket design, a region of packed Beryllium spheres with Helium (or a mixture of noble gases) can be used to provide the necessary temperature drop between the hot solid breeder and cold coolant. The advantage of this blanket design is that by changing the gas pressure or the flow rate (if there is flow), the effective conductivity of the bed can be changed. Therefore, the temperature of the solid breeder material can be

† To whom all correspondence is to be sent.

actively controlled during operation and kept within the allowable temperature window. This provides the flexibility to accommodate any variation of power and/or thermal resistances.

There have been numerous attempts in the past to devise a scheme which determines k_e for packed beds; because of the large volume of literature involved, only a few of these will be mentioned here. Kuni and Smith (1960) and Ogniewicz and Yovanovitch (1978) derived a set of equations for k_e based on one dimensional heat flow in spherical particles. One dimensional models are limited to cases where the solid to gas thermal conductivity ratio (k_s/k_g) is small. Also the empirical constants and fitting parameters included in these models are often difficult to predict. Nozad *et al.* (1985) used volume averaging techniques combined with a numerical and perturbation method to predict k_e. This model does not allow one to determine the influence of gas pressure on k_e and is limited to regions of low k_s/k_g. A different approach suggested by Deissler and Boegli (1958), Wakao and Vortmeyer (1971), and Ades and Peddicord (1982) combines a 2-D unit cell concept with a finite difference scheme to calculate k_e for packed beds. Because of the mesh geometry used in these investigations, the 2-D models are limited to low values of k_s/k_g. A model by Zehner and Schlunder (1972) can calculate the effective medium conductivity for a packed bed as a function of gas pressure, but is not applicable to binary mixtures. Recently, a statistical method for determining k_e was developed by Torquato (1987) for particle beds of arbitrary microstructure, but this model does not account for variation of gas pressure in the particle bed. The key shortcoming in all of the previous models is that they either do not provide reasonable estimates of k_e at high values of k_s/k_g ($\sim$1000) for both single size and binary mixtures of particles, or they fail to do so when gas pressure is changed.

Since the focus of this study is in those regimes, a 2-D unit cell finite difference scheme which also approximates roughnesses at the surface of particles is devised here to handle such cases. Previously developed models do not account for the surface roughness; the importance of this parameter and contact area between particles will also be examined here. This method has the advantage of being applicable to binary (two different sizes) mixtures of particles. The results are compared with the experimental data of Tickle (1990).

2. UNIT CELL

It has been shown by McGeary (1961) that particles in a sphere-pac bed tend to arrange themselves in an orthorhombic formation ($\varepsilon = 39.5\%$). Based on this arrangement, Adnani *et al.* (1989) came up with a 3-D unit cell model which determines the value of k_e. Their study showed that the third dimension (θ) of the unit cell is unimportant and that a 2-D unit cell is sufficient to describe the heat flow in sphere-pac beds. It should be mentioned that near solid boundaries, particles do not form an orthorhombic arrangement. Therefore, this model is only applicable to cases where the layer thickness to particle diameter ratio is larger than 10.

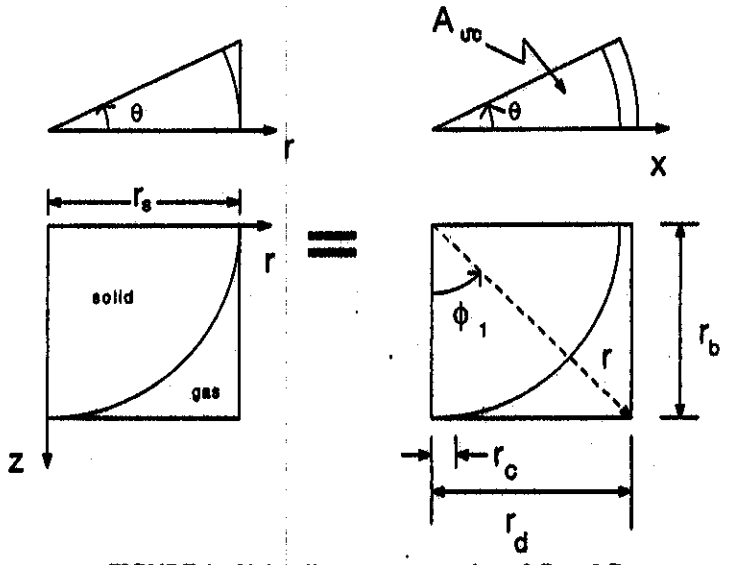

FIGURE 1 Unit cell rearrangement from 3-D to 2-D.

Figure 1 shows the 2-D unit cell where r_d is set based on the bed porosity (ε). This type of unit cell has been used in the past by Deissler and Boegli (1958), Wakao and Vortmeyer (1971), and Ades and Peddicord (1982), but all of the previous authors have used a Cartesian grid inside the unit cell. Since the temperature jump across the solid/gas interface is extremely large at high k_s/k_g, a Cartesian grid may not be the proper approach here. A spherical mesh with variable grid spacing (Figure 2) is more appropriate since near the interface, grid spacings can be chosen small enough to allow for steep gradients, while larger spacings are used elsewhere in the mesh. This type of mesh geometry will be used

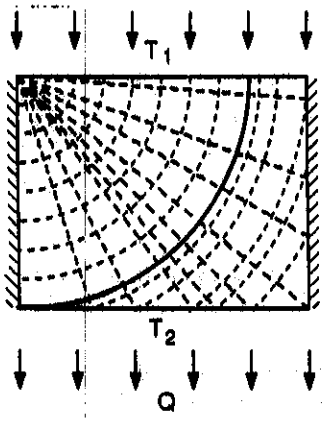

FIGURE 2 Diagram of spherical grid.

in this paper. The governing conduction equation for this geometry is

$$\frac{\partial}{\partial r}\left(r^2 k \frac{\partial T}{\partial r}\right) + \frac{1}{\sin\phi}\frac{\partial}{\partial \phi}\left(k \sin\phi \frac{\partial T}{\partial \phi}\right) = 0 \tag{1}$$

subject to the following boundary conditions:

$$\begin{aligned} @\ \phi = 0 \quad & \frac{\partial T}{\partial \phi} = 0 \\ @\ \phi = \frac{\pi}{2} \quad & T = T_1 \\ \text{for } \phi \le \phi_1 \quad \text{and} \quad r\cos\phi = r_b \quad & T = T_2 \\ \text{for } \phi > \phi_1 \quad \text{and} \quad r\sin\phi = r_d \quad & \frac{\partial T}{\partial x} = 0 \end{aligned} \tag{2}$$

Contact area between the particles is defined by a parameter ρ where

$$\rho = \left(\frac{r_c}{r_s}\right)^2 \tag{3}$$

The influence of this parameter on k_e is important in this study because the beryllium particles in the ITER blanket will experience thermal expansion and radiation swelling as the blanket is operated over time. Particle swelling can change the properties of the bed in two ways. First, the bed porosity will be decreased due to volume expansion and second, contact area between particles will be increased due to the same process. A reduction in ε will tend to increase k_e, but for moderate amount of swelling the effect is believed to be small. Change in contact area though, can have a larger effect depending on the closeness of the particle packing. Increase in contact area will ultimately result in most of the heat flowing through the contact and in the loss of active control of the packed bed k_e through gas pressure adjustment. The influence of contact area on k_e will be examined in more detail in the next section.

To correctly model microscopic roughnesses at the surface of particles, one needs an enormous number of enlarged pictures (i.e. electron micrographs) of particles combined with fairly sophisticated statistical averaging techniques. Such a task is well beyond the scope of this paper. Nevertheless, it is possible to model these roughnesses in a simplified manner. Basically, surface roughnesses will be modeled as cylindrical elements sticking out of the particle surface (Figure 3). Two parameters quantify these cylinders; $(R_1/R_2)^2$ represents the percentage of particle surface area covered by the roughnesses and δ is the average height of the cylindrical elements. At high k_s/k_g, the value of these parameters is chosen so that results from the unit cell model fit the experimental data best. However, as a first approximation, SEM (Scanning Electron Microscope) photographs of the particles used by Tickle (1990) were used to estimate R_1/R_2 and δ.

The unit cell model also has the capability to determine k_e as a function of gas pressure and various particle sizes based on Ades and Peddicord (1982) approach.

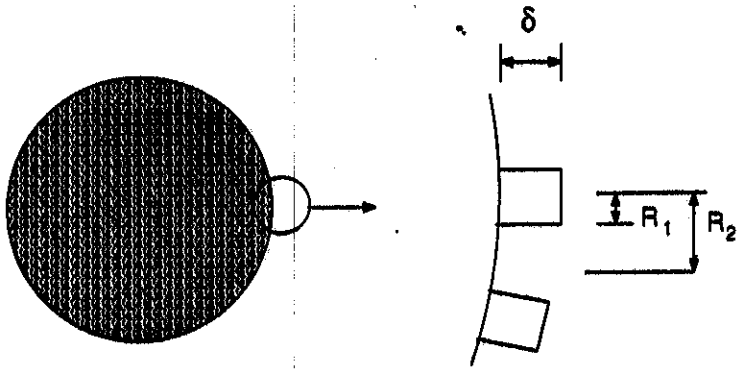

FIGURE 3 Modeling of surface roughness.

This method allows the gas conductivity to change in the following manner

$$k_g = \frac{k_{std}}{1+\sigma} \tag{4}$$

where

$$\sigma = 4\frac{2-\alpha}{\alpha}\frac{\gamma}{\gamma-1}\frac{1}{Pr_g}\frac{\eta_{std}}{P}\frac{T}{273}\frac{1}{d_{gap}} \tag{5}$$

To calculate the effective conductivity, artificial temperatures (T_1, T_2) are specified at the top and bottom part of the unit cell (Figure 2). These temperatures produce an artificial heat flow in the axial (z) direction, from which the effective conductivity can be calculated

$$k_e = \frac{Q}{A_{uc}(T_1 - T_2)}\frac{r_b}{} \tag{6}$$

There is also the capability to model binary mixtures of particles based on the unit cell of Figure 4. The unit cell comprises three regions: the solid region representing the large particles, the homogeneous fine fraction region representing the small particles, and a gas region where the spacing (L_0) between the

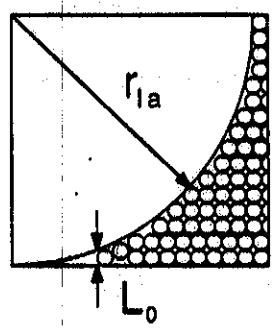

FIGURE 4 Binary mixture of spherical particles.

large particles is too small for the small particles to fit in. The thermal conductivity of the gas in this region is based again on Eqs. (4) and (5). The calculations proceeds as follows: first, k_e for the small (fine) fraction of the mixture is calculated by the single size unit cell model. Next, it is assumed that the region occupied by this small fraction in Figure 4 has that value of k_e distributed homogeneously (the mesh is chosen to accommodate for this). The finite difference code is then used for a second time to calculate an overall value of k_e for the combined binary mixture.

3. COMPARISON WITH EXPERIMENTS

The effective thermal conductivity for single size aluminum particles is shown as a function of gas pressure in Figure 5. The dots represent experimental data from Tickle (1990), while the lines represent results from the model. Parameters R_1/R_2 and δ were chosen as described in the previous section. Two different gases (He and N_2) were used in the experiment to observe the influence of gas properties on k_e. Note that for the Al/He mixture, ($k_s/k_{std} = 1300$), the presence of contact area between particles changes k_e by a maximum of 10%. For the Al/N_2 mixture ($k_s/k_{std} = 7800$), however, the influence of contact area is very significant ($\pm 150\%$) indicating that at high ratios of k_s/k_{std}, most of the heat flows through the contact region. Figure 6 shows the effective thermal conductivity of a packed bed of aluminum powder. Electron micrographs of this powder material show the particles to vary in shape from spherical to potato shaped. Once again surface roughness properties were estimated by examining these micrographs. The agreement between calculations and measurement for the Al/He mixture is excellent, whereas the Al/N_2 mixture results show some deviation ($\pm 15\%$ maximum) from experimental results. This indicates that although the unit cell

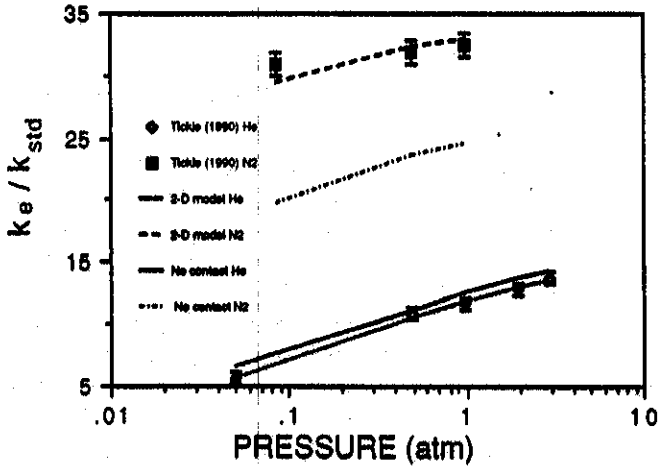

FIGURE 5 Plot of effective thermal conductivity vs gas pressure for Ball Bearings ($e = 37\%$, $d = 5.62 \times 10^{-4}$ m, $\rho = 7 \times 10^{-4}$, $R_1/R_2 = 0.18$, $\delta = 5 \times 10^{-6}$ m).

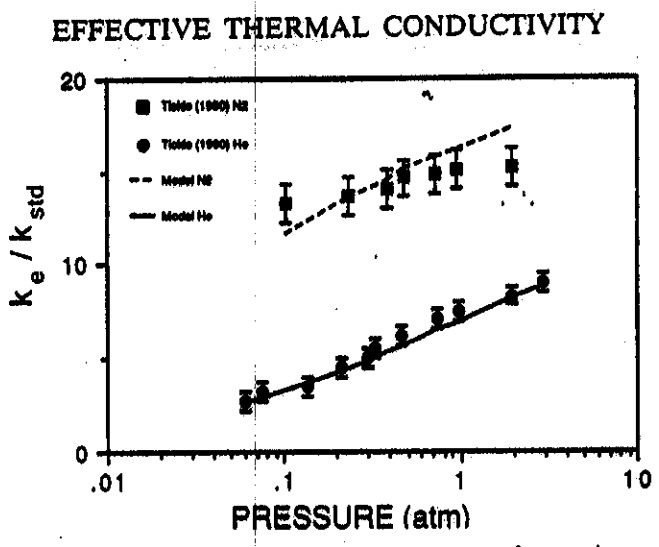

FIGURE 6 Plot of effective thermal conductivity vs gas pressure for powder material ($\varepsilon = 43\%$, $d = 1.2 \times 10^{-4}$ m, $\rho = 1 \times 10^{-4}$, $R_1/R_2 = 0.11$, $\delta = 1 \times 10^{-6}$ m).

model is based on the assumption that the particles are spherical, it provides reasonable estimates for packed beds of particles which are not perfectly spherical for ratios of k_e/k_{std} of the order 1300 or less.

In modeling binary mixtures, the minimum separation distance (L_0 in Figure 4) was assumed to have a value of $d_{sm}/2$. This is a reasonable approximation since the particle bed used by Tickle (1990) was vibrated vigorously so that close packing of particles was achieved. Another key point here is that the surface properties (δ, R_1/R_2) and the contact area parameter (ρ) for each fraction of the binary mixture is kept the same as before (both fractions of binary mixtures were modeled first as single size particle beds to help determine surface properties and contact area parameter). Any modification of these parameters in order to insure agreement with experiments would be unjustified. The binary mixture shown in Figure 7 has a d_{la}/d_{sm} of 45 with a porosity of 15%. Considering the fact that experimental uncertainty is ±10%, excellent agreement with experiments is achieved in the given range of gas pressures. The results shown in Figure 8 ($d_{la}/d_{sm} = 7.5$, $\varepsilon = 18\%$) tend to be somewhat higher than experimental results, but are still within the experimental uncertainty range. McGeary (1961) has noted that below a diameter ratio (d_{la}/d_{sm}) of 7 the value of the packing efficiency ($1 - \varepsilon$) decreases rapidly because the smaller size particles will no longer be arranged in an orthorhombic formation. It is therefore expected that as the value of d_{la}/d_{sm} is decreased the predictions by the model become more and more unreliable. This could explain some of the discrepancy between model predictions and experimental results at $\varepsilon = 18\%$. It is believed that the model is best suited to predict k_e for cases with $d_{la}/d_{sm} \geq 15$ at which the porosity of the binary mixture stays at a value of 15% and both fractions of the mixture are arranged in an orthorhombic fashion. For $7 \leq d_{la}/d_{sm} < 15$, the model predictions tend to be higher than experimental results, but could still be within a reasonable uncertainty range. For $d_{la}/d_{sm} < 7$, the smaller size particles of the mixture are no

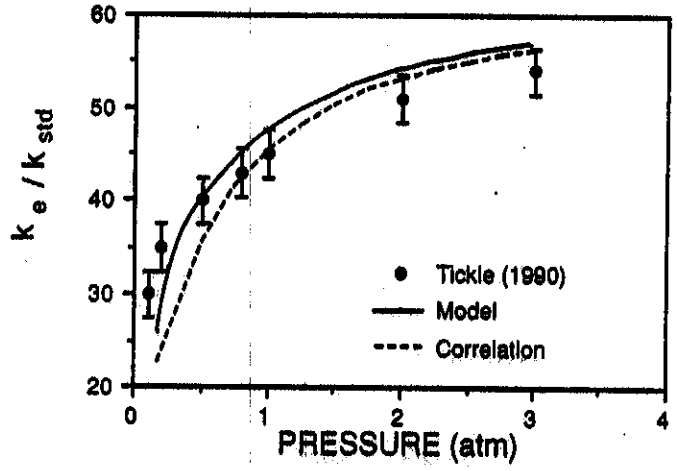

FIGURE 7 Plot of effective conductivity for binary mixture ($\varepsilon = 15\%$, $d_{ln} = 4.2 \times 10^{-3}$ m, $d_{sm} = 1.2 \times 10^{-4}$ m, $\rho_{ln} = 2 \times 10^{-4}$, $\rho_{sm} = 1 \times 10^{-4}$, $(R_1/R_2)_{ln} = 0.18$, $(R_1/R_2)_{sm} = 0.11$, $\delta_{ln} = 2 \times 10^{-5}$ m, $\delta_{sm} = 1 \times 10^{-6}$ m).

longer arranged in an orthorhombic fashion and the model predictions will increasingly diverge from experimental data and, thus, it is not recommended that the model be used for this range of d_{ln}/d_{sm}.

4. DEVELOPMENT OF CORRELATION

Up to this point, the conductivity (k_e) has been calculated for a certain gas at a given pressure with specified particle diameters (d_{ln}/d_{sm}). A non-dimensional

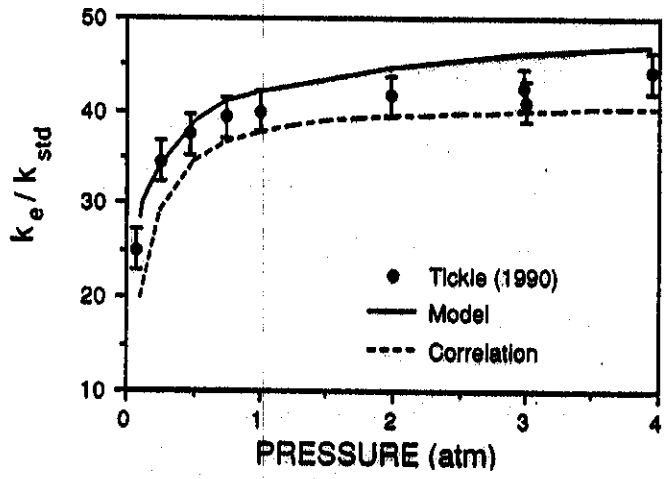

FIGURE 8 Plot of effective conductivity for binary mixture ($\varepsilon = 18\%$, $d_{ln} = 4.2 \times 10^{-3}$ m, $d_{sm} = 5.6 \times 10^{-4}$ m, $\rho_{ln} = 2 \times 10^{-4}$, $\rho_{sm} = 7 \times 10^{-4}$, $(R1/R2)_{ln} = 0.18$, $(R1/R2)_{sm} = 0.18$, $\delta_{ln} = 2 \times 10^{-5}$ m, $\delta_{sm} = 5 \times 10^{-6}$ m).

parametric study was carried out to determine a set of correlations which can be used to estimate k_e for various binary mixtures. Going back to equations 4 and 5, note that σ is the major non-dimensional parameter which effects the value of k_e. Changing the type of gas, gas pressure, temperature and particle size affect k_e by changing the value of σ. Based on this, a new parameter ψ can be introduced:

$$\psi = \frac{2-\alpha}{\alpha}\frac{\gamma}{\gamma-1}\frac{1}{Pr_g}\frac{\eta_{std}}{P}\frac{T}{273}\frac{1}{d_{sm}} \tag{7}$$

Note that d_{sm} is chosen as the characteristic length because it is smaller than d_{ln} and therefore has a more pronounced effect on k_e. For a binary mixture of particles, one can first determine the value of ψ and then use the following correlations to estimate k_e. For $\varepsilon = 15\%$ and $1 \le k_s/k_{std} \le 20$:

$$\frac{k_e}{k_{std}} = A_1 + B_1\left(\frac{k_s}{k_{std}}\right) + C_1\left(\frac{k_s}{k_{std}}\right)^2 \tag{8}$$

if $20 < k_s/k_{std} \le 1300$:

$$\frac{k_e}{k_{std}} = D_1 + E_1 \log\left(\frac{k_s}{k_{std}}\right) \tag{9}$$

Similarly for $\varepsilon = 18\%$ and $1 \le k_s/k_{std} \le 20$:

$$\frac{k_e}{k_{std}} = A_2 + B_2\left(\frac{k_s}{k_{std}}\right) + C_2\left(\frac{k_s}{k_{std}}\right)^2 \tag{10}$$

if $20 < k_s/k_{std} \le 1300$:

$$\frac{k_e}{k_{std}} = D_2 + E_2 \log\left(\frac{k_s}{k_{std}}\right) \tag{11}$$

the coefficients A_n, B_n, C_n, D_n and E_n are defined in the appendix. An important point about these correlations is that they were derived by assuming zero contact area between particles. In practice, contact area is always larger than zero, therefore, actual value of k_e would be larger when compared with correlations. To check the accuracy of these correlations, results are plotted in Figures 7 and 8. Note that even at high k_s/k_{std} ($\sim$1300), good agreement with experimental data is achieved for a range of gas pressures. Therefore, these correlations provide a lower bound estimation of k_e for binary mixtures when $1 < k_s/k_{std} \le 1300$. For larger values of k_s/k_{std}, contact area plays a more significant role (on magnitude of k_e) and a reasonable estimation of ρ and surface properties is required. The computer code can provide a better estimation of k_e at high conductivity ratios since it can account for surface properties and contact area.

5. INFLUENCE OF CONTACT AREA AND ROUGHNESS

The last issue which will be investigated here is the effect of particle swelling on k_e. It was mentioned earlier that particle swelling will mainly influence k_e by

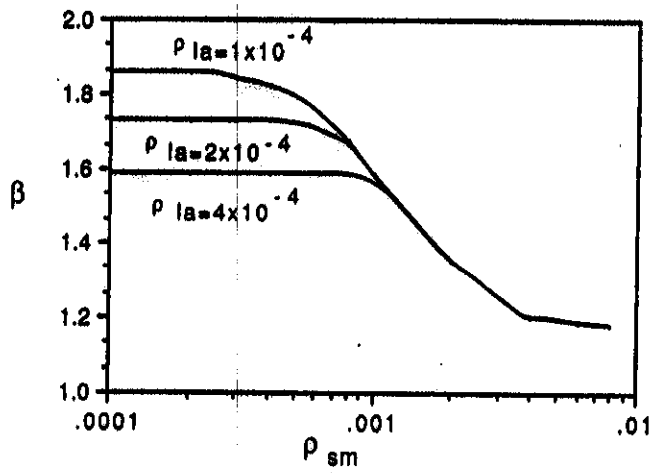

FIGURE 9 Influence of contact area on active control of effective conductivity for binary mixture ($e = 15\%$).

increasing the contact area between particles. To investigate this, the parameter β is plotted as a function of ρ_{sm} for different values of ρ_{la} (Figure 9). Surface properties of the particles in this binary mixture are those shown in Figure 7. β is the ratio of k_e at 2 atm to k_e at 0.2 atm and represents the amount of active control of k_e which the packed bed provides through gas pressure adjustment. Note that a small contact area for both particle sizes provides the largest level of controllability on k_e. This makes sense because when the contact area is small, most of the heat transfer takes place through the solid/gas interface; hence gas pressure by influencing the gas thermal conductivity can significantly affect k_e. As the contact area is increased, β is decreased because more heat is transferred through the contact region and the influence of gas pressure on k_e is thereby reduced.

Another important parameter here is the magnitude of roughness height (δ) at the particle surface. Influence of this parameter on controllability parameter (β) of powder material is shown in Figure 10. A large δ would cause the contact resistance between the particles to be larger, thereby reducing the amount of heat flow through the contact area. This mechanism leads to a larger level of controllability for the packed bed which is desirable here.

Henceforth, in design of packed beds (such as the ITER blanket design) where control of k_e by gas pressure adjustment is an objective, it is advantageous to use particles with rough surface characteristics. Nonetheless, it must be noted that while controllability increases with roughness, the magnitude of effective conductivity tends to decrease. Thus, for cases where high k_e and controllability are both required, a trade off between the two effects exist. One also has to consider the long term effects of particle swelling on the controllability parameter (β) which becomes increasingly important at high solid/gas conductivity ratios.

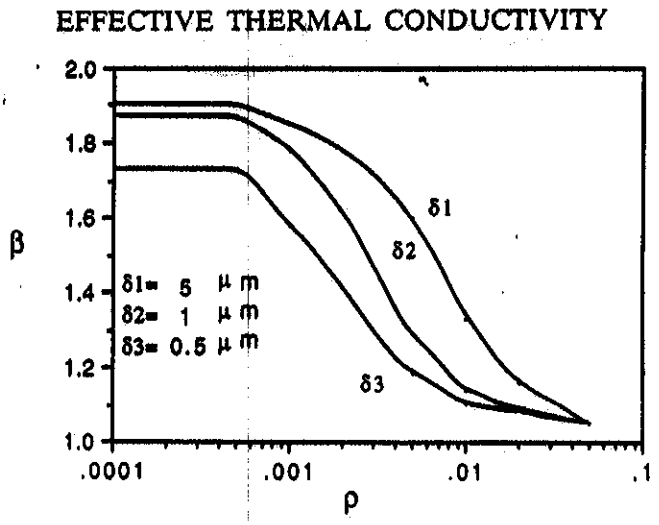

FIGURE 10 Influence of roughness height on active controllability of the powder material ($\varepsilon = 43\%$).

6. CONCLUSIONS

A model for calculating the effective thermal conductivity of single size and binary mixtures of spherical particles as a function of gas pressure in the range $k_s/k_{std} \leq 1300$ was developed.

This model was also shown to be applicable to packed powder beds. It was demonstrated that if $k_s/k_{std} \leq 1300$, contact area does not change k_e by more than 15% for both single size and binary mixtures. Based on this, a set of correlations for effective conductivity of binary mixtures with zero contact area between particles was derived. These correlations provide a lower bound estimate of k_e in the range $k_s/k_{std} \leq 1300$. For larger values of k_s/k_{std}, influence of particle shape and contact area on k_e becomes more significant and the model can provide a better estimation of k_e if information on surface properties is available.

For binary mixtures it was shown that particle swelling and increase of contact area can reduce the amount of available active controllability on k_e.

ACKNOWLEDGEMENTS

This work was supported by the U.S. Department of Energy under contracts #DE-FG03-86ER52123 and #DE-FG03-86ER14033.

NOMENCLATURE

A_n	coefficients defined in Eq. (a1, a6)
A_{uc}	Unit cell area in Figure 1

B_n	coefficients defined in Eq. (a2, a7)
C_n	coefficients defined in Eq. (a3, a8)
C_p	specific heat at constant pressure
C_v	specific heat at constant volume
d	particle diameter in packed bed
d_{gap}	gap thickness (Eq. (5))
D_n	coefficients defined in Eqs. (a4, a9)
E_n	coefficients defined in Eqs. (a5, a10)
k	thermal conductivity
L_0	minimum separation distance (Fig. 4)
P	gas pressure
Pr	Prandtl number
Q	heat flow in the axial direction
r	radial coordinate
r_b	see Figure 1
r_c	contact radius (Figure 1)
r_d	see Figure 1
r_s	particle radius in packed bed
$(R_1/R_2)^2$	percentage of surface area covered by roughnesses (Figure 3)
T	temperature
x	Cartesian coordinate
z	axial direction

Greek

α	thermal accommodation coefficient
β	k_r(at $P = 2$ atm)/k_r (at $P = 0.2$ atm)
γ	specific heat ratio (C_p/C_v)
δ	roughness height (Figure 3)
ε	porosity
η	mean free path of gas molecule
θ	tangential coordinate
ρ	contact area parameter (Eq. (3))
σ	see Eq. (4)
ϕ	azimuthal coordinate
ψ	parameter defined in Eq. (7)

Subscripts

e	effective value for the packed bed
g	gas
la	large
s	solid
sm	small
std	condition for gas at 1 atm and 273 K

REFERENCES

Abdou, M.A., Raffray, A.R., Gorbis, Z.R., Tillack, M.S., Watanabe, Y., Ying, A.Y., Youssef, M.Z., and Fujimura, K., "A Helium-Cooled Solid Breeder Concept for the Tritium-Producing Blanket of the International Thermonuclear Experimental Reactor," *Fusion Technology*, **15**, 2, pt. 1, 166–182 (1989).

Ades, M.J., and Peddicord, K.L., "A Model for Effective Thermal Conductivity of Unrestructured Sphere-Pac Fuel," *Nuc. Sci. and Eng.*, **81**, 540–550 (1982).

Adnani, P., Raffray, A.R., Abdou, M.A., and Catton, I., "Modeling of Effective Thermal Conductivity for a Packed Bed," UCLA FNT-29, University of California, Los Angeles (1989).

Cheng, P., "Heat Transfer in Geothermal Systems," *Advances in Heat Transfer*, Hartnett, J., and Irvine, T.F. eds., Academic Press, pp. 1–105 (1978).

Deissler, R.G., and Boegli, J.S., "An Investigation of Effective Thermal Conductivities of Powders in Various Gases," *Trans. ASME.*, **80**, 1417–1425 (1958).

Friedman, M.H., *Principles and models of biological transport*, Springer-Verlag, Berlin (1986).

Kuni, D., and Smith, J.M., "Heat Transfer Characteristics of Porous Rocks," *A.I.Ch.E. Journal*, **6**, 1, 71–78 (1960).

Luikov, A.V., *Heat and Mass Transfer*, (English Translation), MIR Publishers, Moscow (1980).

McGeary, R.K., "Mechanical Packing of Spherical Particles," *J. Amer. Ceramic Soc.*, **44**, 10, 513–522 (1961).

Nozad, I., Carbonell, R.G., and Whitaker, S., "Heat Conduction in Multiphase Systems-1 Theory and experiment for Two-phase systems," *Chem. Eng. Science*, **40**, 5, 843–855 (1985).

Ogniewicz, Y., and Yovanovitch, M.M., "Effective Conductivity of Regularly Packed Spheres: Basic Cell Model with Construction," *AIAA Prog. Astronautics and Aeronautics*, **60**, 209–228 (1978).

Sommerton, C.W., and Robers, J., "Computer Simulation of a Natural Convection driven Packed Bed of An Oxide Coating," ASME Proc. 1988 National Heat Transfer Conf., HTD-Vol. 96, 1988, pp. 379–384 (1988).

Tickle, C.E., "Measurement of the Thermal Conductivity of Metal–Gas Particle Beds for Solid Breeder Blankets," UCLA-FNT-34, University of California, Los Angeles (1990).

Torquato, S., "Thermal Conductivity of Disordered Heterogeneous Media from the Microstructure," *Reviews in Chem. Eng.*, **4**, 3, 151–204 (1987).

Wakao, N., and Vortmeyer, D., "Pressure dependency of effective thermal conductivity of packed beds," *Chem. Eng. Science*, **26**, 1753–1765 (1971).

Zehner, P., and Schlunder, E.U., "Einfluß der Warmestrahlung und des Druckes auf den Warmetransport in nicht durchstromten Schuttungen," *Chemie. Ing. Tech.*, **44**, 23, 1303–1308 (1972).

APPENDIX

The following coefficients are valid in the range $\psi \leq 0.125$ and $1 \leq k_s/k_{std} \leq 1000$. Note that these are based on the assumption of zero contact area between the particles.

$$A_1 = 0.37 + 1.62\psi - 6.9\psi^2 \qquad \text{(a1)}$$

$$B_1 = 0.79 - 1.22\psi \tag{a2}$$

$$C_1 = 1.3 \times 10^{-2} \tag{a3}$$

$$D_1 = -34.3 + 1050\psi - 1.25 \times 10^4\psi^2 + 4.9 \times 10^4\psi^3 \tag{a4}$$

$$E_1 = 31.4 - 677\psi + 7680\psi^2 - 3 \times 10^4\psi^3 \tag{a5}$$

$$A_2 = 0.44 + 1.97\psi - 27\psi^2 + 150\psi^3 \tag{a6}$$

$$B_2 = 0.7 \tag{a7}$$

$$C_2 = -1.3 \times 10^{-2} \tag{a8}$$

$$D_2 = -15.4 + 760\psi - 9710\psi^2 + 3.8 \times 10^4\psi^3 \tag{a9}$$

$$E_2 = 18.2 - 500\psi + 5920\psi^2 - 2.28 \times 10^4\psi^3 \tag{a10}$$

for $\psi < 2.5 \times 10^{-4}$ use the value corresponding to $\psi = 2.5 \times 10^{-4}$.